

Epoxidation of Alkenes with Hydrogen Peroxide Catalyzed by Selenium-Containing Dinuclear Peroxotungstate and Kinetic, Spectroscopic, and Theoretical Investigation of the Mechanism

Keigo Kamata,^{†,‡} Ryo Ishimoto,[†] Tomohisa Hirano,[†] Shinjiro Kuzuya,[†] Kazuhiro Uehara,^{†,‡} and Noritaka Mizuno^{*,†,‡}

[†]Department of Applied Chemistry, School of Engineering, The University of Tokyo, 7-3-1 Hongo, Bunkyo-ku, Tokyo 113-8656, Japan, and [‡]Core Research for Evolutional Science and Technology (CREST), Japan Science and Technology Agency (JST), 4-1-8 Honcho, Kawaguchi, Saitama 332-0012, Japan

Received December 2, 2009

The dinuclear peroxotungstate with a SeO_4^{2-} ligand, $(\text{TBA})_2[\text{SeO}_4\{\text{WO}(\text{O}_2)_2\}_2]$ (**I**; $\text{TBA}=[(\text{n-C}_4\text{H}_9)_4\text{N}]^+$), could act as an efficient homogeneous catalyst for the selective oxidation of various kinds of organic substances such as olefins, alcohols, and amines with H_2O_2 as the sole oxidant. The turnover frequency (TOF) was as high as 210 h^{-1} for the epoxidation of cyclohexene catalyzed by **I** with H_2O_2 . The catalyst was easily recovered and reused with maintenance of the catalytic performance. The SeO_4^{2-} ligand in **I** played an important role in controlling the Lewis acidity of the peroxotungstates, which significantly affects their electrophilic oxygen-transfer reactivity. Several kinetic and spectroscopic results showed that the present catalytic epoxidation included the following two steps: (i) formation of the subsequent peroxo species $[\text{SeW}_m\text{O}_n]^{q-}$ (**II**; $m=1$ and 2) by the reaction of **I** with an olefin and (ii) regeneration of **I** by the reaction of **II** with H_2O_2 . Compound **I** was the dominant species under steady-state turnover conditions. The reaction rate for the catalytic epoxidation showed a first-order dependence on the concentrations of olefin and **I** and a zero-order dependence on the concentration of H_2O_2 . The rate of the stoichiometric epoxidation with **I** agreed well with that of the catalytic epoxidation with H_2O_2 by **I**. All of these kinetic and spectroscopic results indicate that oxygen transfer from **I** to the $\text{C}=\text{C}$ double bond is the rate-determining step. The computational studies support that the oxygen-transfer step is the rate-determining step.

Introduction

Selective oxygen transfer to organic substances with H_2O_2 as a terminal oxidant is an important reaction in industry and synthetic chemistry because of its high content of active

oxygen species and coproduction of only water.¹ Over the past few decades, homogeneous and heterogeneous transition-metal catalysts such as Ti ,² V ,³ Fe ,⁴ Mn ,⁵ W ,⁶ Re ,⁷ and Pt ⁸ for H_2O_2 -based oxidation have been developed. Notably, the Lewis acid character of the metal catalysts plays an important role in the activation of H_2O_2 and/or substrate

*To whom correspondence should be addressed. E-mail: tmizuno@mail.ecc.u-tokyo.ac.jp. Tel.: +81-3-5841-7272. Fax: +81-3-5841-7220.

(1) (a) Sheldon, R. A.; Kochi, J. K. *Metal Catalyzed Oxidations of Organic Compounds*; Academic Press: New York, 1981. (b) Hill, C. L. In *Advances in Oxygenated Processes*; Baumstark, A. L., Ed.; JAI Press: London, 1988; Vol. 1; pp 1–30. (c) Hudlucky, M. *Oxidations in Organic Chemistry*; ACS Monograph Series; American Chemical Society: Washington, DC, 1990. (d) Bäckvall, J.-E. *Modern Oxidation Methods*; Wiley-VCH: Weinheim, Germany, 2004.

(2) (a) Notari, B. *Adv. Catal.* **1996**, *41*, 253. (b) Arends, I. W. C. E.; Sheldon, R. A.; Wallau, M.; Schuchardt, U. *Angew. Chem., Int. Ed. Engl.* **1997**, *36*, 1144. (c) De Vos, D. E.; Sels, B. F.; Jacobs, P. A. *Adv. Synth. Catal.* **2003**, *345*, 457. (d) Sawada, Y.; Matsumoto, K.; Katsuki, T. *Angew. Chem., Int. Ed.* **2007**, *46*, 4559.

(3) (a) Ligtienbarg, A. G. J.; Hage, R.; Feringa, B. L. *Coord. Chem. Rev.* **2003**, *237*, 89. (b) Carter-Franklin, J. N.; Butler, A. J. *Am. Chem. Soc.* **2004**, *126*, 15060. (c) Nakagawa, Y.; Kamata, K.; Kotani, M.; Yamaguchi, K.; Mizuno, N. *Angew. Chem., Int. Ed.* **2005**, *44*, 5136.

(4) (a) White, M. C.; Doyle, A. G.; Jacobsen, E. N. *J. Am. Chem. Soc.* **2001**, *123*, 7194. (b) Chen, K.; Costas, M.; Que, L., Jr. *J. Chem. Soc., Dalton Trans.* **2002**, 672.

(5) (a) Battioni, P.; Renaud, J. P.; Bartoli, J. F.; Reina-Artiles, M.; Fort, M.; Mansuy, D. *J. Am. Chem. Soc.* **1988**, *110*, 8462. (b) Sibbons, K. F.; Shastri, K.; Watkinson, M. *Dalton Trans.* **2006**, 645.

(6) (a) Noyori, R.; Aoki, M.; Sato, K. *Chem. Commun.* **2003**, 1977. (b) Brégeault, J.-M. *Dalton Trans.* **2003**, 3289. (c) Mizuno, N.; Yamaguchi, K.; Kamata, K. *Coord. Chem. Rev.* **2005**, *249*, 1944.

(7) (a) Romao, C. C.; Kühn, F. E.; Herrmann, W. A. *Chem. Rev.* **1997**, *97*, 3197. (b) Rudolph, J.; Reddy, K. L.; Chiang, J. P.; Sharpless, K. B. *J. Am. Chem. Soc.* **1997**, *119*, 6189.

(8) (a) Colladon, M.; Scarso, A.; Sgarbossa, P.; Michelin, R. A.; Strukul, G. J. *Am. Chem. Soc.* **2006**, *128*, 14006. (b) Colladon, M.; Scarso, A.; Sgarbossa, P.; Michelin, R. A.; Strukul, G. J. *Am. Chem. Soc.* **2007**, *129*, 7680.

(9) (a) Lane, B. S.; Burgess, K. *Chem. Rev.* **2003**, *103*, 2457. (b) Corma, A.; Garcia, H. *Chem. Rev.* **2003**, *103*, 4307. (c) ten Brink, G.-J.; Arends, I. W. C. E.; Sheldon, R. A. *Chem. Rev.* **2004**, *104*, 4105. (d) Boronat, M.; Concepcion, P.; Corma, A.; Renz, M. *Catal. Today* **2007**, *121*, 39. (e) Thiel, W. R.; Eppinger, J. *Chem.—Eur. J.* **1997**, *3*, 696. (f) Arends, I. W. C. E.; Sheldon, R. A. *Top. Catal.* **2002**, *19*, 133.

for the catalytic oxygen-transfer reactions (e.g., epoxidation and Baeyer–Villiger reaction) and the high activity correlates well with the high Lewis acidity of metal centers.^{9,10} Therefore, the electronic and steric control of catalytically active centers is one of the most important points in achieving the desired chemo-, regio-, diastereo-, and stereoselectivity toward products.

Polyoxometalates are early-transition-metal oxygen anion clusters that have been applied to various fields such as structural chemistry, analytical chemistry, surface science, medicine, electrochemistry, photochemistry, and catalysis.¹¹ Polyoxometalates have the following advantages as oxidation catalysts: (a) The redox and acid–base properties can be controlled by changes in the chemical composition, (b) they are not susceptible to oxidative and thermal degradation in comparison with organometallic complexes, and (c) the catalytically active sites can be designed at the atomic and/or molecular levels. Therefore, many catalytic H₂O₂-based oxidations by polyoxometalates such as peroxometalates,¹²

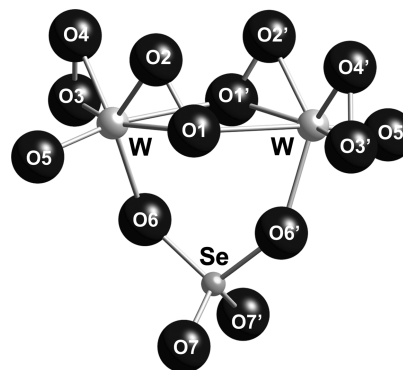


Figure 1. Proposed structure of the anionic part of I.

lacunary polyoxometalates,¹³ and transition-metal-substituted polyoxometalates¹⁴ have been developed.

Recently, we have reported the highly efficient epoxidation of homoallylic and allylic alcohols and oxidation of sulfides with H₂O₂ catalyzed by a selenium-containing dinuclear peroxotungstate, (TBA)₂[SeO₄{WO(O₂)₂}₂] (I; TBA = [(n-C₄H₉)₄N]⁺; Figure 1).¹⁵ The nature of the heteroatoms in the di- and tetranuclear peroxotungstates with XO₄^{n−} ligands (X = Se^{VI}, S^{VI}, As^V, P^V, Si^{IV}, etc.) was crucial in controlling the Lewis acidity of the peroxotungstates, which significantly affects their electrophilic oxygen-transfer reactivity. In this paper, we report full details of the catalytic performance of I for the H₂O₂-based oxidation of various organic substrates, including olefins, alcohols, and amines, and investigate the kinetic and mechanistic aspects of the I-catalyzed epoxidation system.

Experimental Section

Materials. Acetonitrile (Kanto Chemical) and dichloromethane (Kanto Chemical) were purified by The Ultimate Solvent System (Glass Contour Company) prior to use.¹⁶ Substrates were purified according to the reported procedure.¹⁷ Deuterated solvents (CD₃CN, CDCl₃, and D₂O) were purchased from Acros and used as received. Tungstic acid (Wako Chemical), H₂SeO₄ (Kanto Chemical, 80% aqueous solution), tetra-*n*-butylammonium nitrate (Wako Chemical), and H₂O₂ (Kanto Chemical, 30% aqueous solution) were used as received.

Instruments. IR spectra were measured on a Jasco FT/IR-460 spectrometer Plus using KCl disks. Raman spectra were recorded on a Jasco NR-1000 spectrometer with excitation at 532.36 nm using a JUNO 100 green laser (Showa Optronics Co., Ltd.). UV–vis spectra were recorded on a Jasco V-570 spectrometer. NMR spectra were recorded on a JEOL JNM-EX-270 spectrometer (¹H, 270.0 MHz; ¹³C, 67.80 MHz; ⁷⁷Se, 51.30 MHz; ¹⁸³W, 11.20 MHz) by using 5 mm tubes (for ¹H and ¹³C) or 10 mm tubes (for ⁷⁷Se and ¹⁸³W). Chemical shifts (δ) were reported in ppm downfield from SiMe₄ (solvent, CDCl₃) for ¹H and ¹³C NMR spectra, Me₂Se (solvent, DMF-*d*₇) for ⁷⁷Se NMR spectra, and 2 M Na₂WO₄ (solvent, D₂O) for ¹⁸³W NMR spectra. Gas chromatography (GC) analyses were performed on a Shimadzu GC-2014 gas chromatograph with a flame ionization detector equipped with an InertCap 5 capillary column (internal diameter = 0.25 mm; length = 60 m) and a Shimadzu

(10) *Catalysis: An Integrated Approach to Homogeneous, Heterogeneous and Industrial Catalysis*; Moulijn, J. A., van Leeuwen, P. W. N. M., van Santen, R. A., Eds.; Elsevier: Amsterdam, The Netherlands, 1993.

(11) (a) Pope, M. T. *Heteropoly and Isopoly Oxometalates*; Springer-Verlag: Berlin, 1983. (b) Hill, C. L.; Chrisina, C.; Prosser-McCarthy, M. *Coord. Chem. Rev.* **1995**, *143*, 407. (c) Okuhara, T.; Mizuno, N.; Misono, M. *Adv. Catal.* **1996**, *41*, 113. (d) Neumann, R. *Prog. Inorg. Chem.* **1998**, *47*, 317. (e) Thematic issue on “Polyoxometalates”: Hill, C. L. *Chem. Rev.* **1998**, *98*, 1–389. (f) Kozhevnikov, I. V. *Catalysis by Polyoxometalates*; John Wiley & Sons: Chichester, U.K., 2002. (g) Pope, M. T. In *Comprehensive Coordination Chemistry II*; McCleverty, J. A., Meyer, T. J., Eds.; Elsevier Pergamon: Amsterdam, The Netherlands, 2004; Vol. 4; p 635. (h) Hill, C. L. In *Comprehensive Coordination Chemistry II*; McCleverty, J. A., Meyer, T. J., Eds.; Elsevier Pergamon: Amsterdam, The Netherlands, 2004; Vol. 4; p 679. (i) Mizuno, N.; Kamata, K.; Yamaguchi, K. In *Surface and Nanomolecular Catalysis*; Richards, R., Ed.; Taylor and Francis Group: New York, 2006; p 463. (j) Mizuno, N.; Kamata, K.; Uchida, S.; Yamaguchi, K. In *Modern Heterogeneous Oxidation Catalysis*; Mizuno, N., Ed.; Wiley-VCH: Weinheim, Germany, 2009; p 185.

(12) (a) Ishii, Y.; Yoshida, T.; Yamawaki, K.; Ogawa, M. *J. Org. Chem.* **1988**, *53*, 5549. (b) Venturello, C.; D'Aloisio, R.; Bart, J. C. J.; Ricci, M. *J. Mol. Catal.* **1985**, *32*, 107. (c) Dengel, A. C.; Griffith, W. P.; Parkin, B. C. *J. Chem. Soc., Dalton Trans.* **1993**, 2683. (d) Duncan, D. C.; Chambers, R. C.; Hecht, E.; Hill, C. L. *J. Am. Chem. Soc.* **1995**, *117*, 681. (e) Kamata, K.; Yamaguchi, K.; Hikichi, S.; Mizuno, N. *Adv. Synth. Catal.* **2003**, *345*, 1193. (f) Kamata, K.; Yamaguchi, K.; Mizuno, N. *Chem.—Eur. J.* **2004**, *10*, 4728. (g) Kamata, K.; Kuzuya, S.; Uehara, K.; Yamaguchi, S.; Mizuno, N. *Inorg. Chem.* **2007**, *46*, 3768. (h) Brégeault, J.-M.; Vennat, M.; Salles, L.; Piquemal, J.-Y.; Mahla, Y.; Briot, E.; Bakala, P. C.; Atlamsani, A.; Thouvenot, R. *J. Mol. Catal. A: Chem.* **2006**, *250*, 177.

(13) (a) Kamata, K.; Yonehara, K.; Sumida, Y.; Yamaguchi, K.; Hikichi, S.; Mizuno, N. *Science* **2003**, *300*, 964. (b) Kamata, K.; Nakagawa, Y.; Yamaguchi, K.; Mizuno, N. *J. Catal.* **2004**, *224*, 224. (c) Kamata, K.; Kotani, M.; Yamaguchi, K.; Hikichi, S.; Mizuno, N. *Chem.—Eur. J.* **2007**, *13*, 639. (d) Musaev, D. G.; Morokuma, K.; Geletii, Y. V.; Hill, C. L. *Inorg. Chem.* **2004**, *43*, 7702. (e) Prabhakar, R.; Morokuma, K.; Hill, C. L.; Musaev, D. G. *Inorg. Chem.* **2006**, *45*, 5703. (f) Sartorel, A.; Carraro, M.; Bagno, A.; Scorrano, G.; Bonchio, M. *Angew. Chem., Int. Ed.* **2007**, *46*, 3255. (g) Carraro, M.; Sandei, L.; Sartorel, A.; Scorrano, G.; Bonchio, M. *Org. Lett.* **2006**, *8*, 3671. (h) Phan, T. D.; Kinch, M. A.; Barker, J. E.; Ren, T. *Tetrahedron Lett.* **2005**, *46*, 397. (i) Ishimoto, R.; Kamata, K.; Mizuno, N. *Angew. Chem., Int. Ed.* **2009**, *48*, 8900.

(14) (a) Neumann, R.; Gara, M. *J. Am. Chem. Soc.* **1995**, *117*, 5066. (b) Bösing, M.; Nöh, A.; Loose, L.; Krebs, B. *J. Am. Chem. Soc.* **1998**, *120*, 7252. (c) Ritorto, M. D.; Anderson, T. M.; Neiwert, W. A.; Hill, C. L. *Inorg. Chem.* **2004**, *43*, 44. (d) Sloboda-Rozner, D.; Alsters, P. L.; Neumann, R. *J. Am. Chem. Soc.* **2003**, *125*, 5280. (e) Sloboda-Rozner, D.; Witte, P.; Alsters, P. L.; Neumann, R. *Adv. Synth. Catal.* **2004**, *346*, 339. (f) Zhang, X.; Chen, Q.; Duncan, D. C.; Campana, C. F.; Hill, C. L. *Inorg. Chem.* **1997**, *36*, 4208. (g) Anderson, T. M.; Zhang, X.; Hardcastle, K. I.; Hill, C. L. *Inorg. Chem.* **2002**, *41*, 2477. (h) Zhang, X.; Anderson, T. M.; Chen, Q.; Hill, C. L. *Inorg. Chem.* **2001**, *40*, 418. (i) Mizuno, N.; Nozaki, C.; Kiyoto, I.; Misono, M. *J. Am. Chem. Soc.* **1998**, *120*, 9267. (j) Ben-Daniel, R.; Khenkin, A. M.; Neumann, R. *Chem.—Eur. J.* **2000**, *6*, 3722.

(15) (a) Kamata, K.; Hirano, T.; Kuzuya, S.; Mizuno, N. *J. Am. Chem. Soc.* **2009**, *131*, 6997. (b) Kamata, K.; Hirano, T.; Mizuno, N. *Chem. Commun.* **2009**, 3958.

(16) Pangborn, A. B.; Giardello, M. A.; Grubbs, R. H.; Rosen, R. K.; Timmers, F. J. *Organometallics* **1996**, *15*, 1518.

(17) Perrin, D. D.; Armarego, W. L. F. *Purification of Laboratory Chemicals*, 3rd ed.; Pergamon Press: Oxford, U.K., 1988.

GC-17A gas chromatograph with a flame ionization detector equipped with an InertCap Pure-WAX capillary column (internal diameter = 0.25 mm; length = 30 m).

Synthesis and Characterization of $[(n\text{-C}_4\text{H}_9)_4\text{N}]_2[\text{SeO}_4\{\text{WO}(\text{O}_2)_2\}_2]^{2-}$ (I). The TBA salt derivative of $[\text{SeO}_4\{\text{WO}(\text{O}_2)_2\}_2]^{2-}$ was synthesized according to the reported procedure.¹⁵ Full details of the synthesis and characterization of **I** are shown in the Supporting Information (Figures S1–S5).

Procedure for Catalytic Oxidation. Catalytic oxidation of various organic substrates was carried out in a 30-mL glass vessel containing a magnetic stir bar. All products were identified by a comparison of the GC retention time, mass spectra, and NMR spectra with those of the authentic samples. A typical procedure for catalytic oxidation was as follows: **1a** (5 mmol), acetonitrile (6 mL), and 30% aqueous H_2O_2 (1 mmol) were charged in the reaction vessel. The reaction was initiated by the addition of **I** (10 μmol), and the reaction solution was periodically analyzed. H_2O_2 remaining after the reaction was analyzed by $\text{Ce}^{3+/4+}$ titration.¹⁸ The products (**10b**,¹⁹ **11b**,¹⁹ and **14b**²⁰) are known and identified by a comparison of their ^1H and ^{13}C NMR signals with the literature data. **10b**: ^1H NMR (270 MHz, CDCl_3 , 298 K, TMS) δ 6.68 (t, J = 5.9 Hz, 1H), 3.76 (t, J = 7.0 Hz, 2H), 2.48 (dt, J = 5.9 and 6.8 Hz, 2H), 1.92–1.86 (m, 2H), 1.60–1.52 (m, 2H), 1.40–1.32 (m, 2H), 0.98 (t, J = 7.3 Hz, 3H), 0.96 (t, J = 7.6 Hz, 3H); $^{13}\text{C}\{^1\text{H}\}$ NMR (67.5 MHz, CDCl_3 , 298 K, TMS) δ 139.5, 65.2, 29.5, 28.6, 19.7, 19.1, 14.0, 13.6. **11b**: ^1H NMR (270 MHz, CDCl_3 , 298 K, TMS) δ 7.76 (s, 1H), 7.30–7.10 (m, 4H), 4.06 (dt, J = 0.8 and 7.6 Hz, 2H), 3.18 (t, J = 7.3 Hz, 2H); $^{13}\text{C}\{^1\text{H}\}$ NMR (67.5 MHz, CDCl_3 , 298 K, TMS) δ 134.2, 120.1, 129.4, 128.4, 127.7, 127.3, 125.5, 58.0, 27.8. **14b**: ^1H NMR (270 MHz, CDCl_3 , 298 K, TMS) δ 3.79–3.64 (m, 2H), 3.61–3.45 (m, 2H), 1.90–1.77 (m, 3H), 1.62–1.44 (m, 1H), 1.04 (d, J = 6.2 Hz, 3H); $^{13}\text{C}\{^1\text{H}\}$ NMR (67.5 MHz, CD_3CN , 298 K, TMS) δ 84.4, 70.5, 68.5, 28.3, 26.8, 19.3.

Recovery of Catalyst and Recycle Experiments. The reaction conditions for the first run were as follows: **I** (10 μmol), **3a** (5 mmol), 30% aqueous H_2O_2 (1 mmol), CH_3CN (6 mL), 298 K. The corresponding epoxide **3b** was obtained in 99% yield for 100 min. After epoxidation of **3a** was completed, acetonitrile was removed by evaporation, followed by the addition of diethyl ether (20 mL). The precipitated catalyst was collected (98% recovery), washed with diethyl ether (ca. 20 mL \times 2), and dried in vacuo prior to being recycled. Epoxidation in the presence of the recovered **I** proceeded with almost the same yield and selectivity as those observed for the first run, and **3b** was obtained in 96% yield.

Quantum Chemical Calculations. The calculations were carried out at the B3LYP level of theory²¹ with 6-31+G(d,p) basis sets for H, C, and O atoms and the double- ξ quality basis sets with effective core potentials proposed by Hay and Wadt²² for Se and W atoms. The entire structure of peroxotungstate was used as a model in the calculations, and the overall charge of the system was 2-. Ethylene was used as a model substrate. All of the geometries were optimized without symmetry restrictions. Transition-state structures were searched by numerically estimating the matrix of second-order energy derivatives at every optimization step and by requiring exactly one eigenvalue of this matrix to be negative. The optimized geometries are shown in Table S1 and Figures 5 and S6 in the Supporting Information. The zero-point vibrational energies were not included.

All calculations were performed with the Gaussian03 program package.²³

Results and Discussion

Catalytic Oxidation with H_2O_2 by **I.** The catalytic activity of **I** for epoxidation of cyclohexene (**1a**) was compared with those of the Se and W catalysts (Table 1). Among the catalysts tested, **I** showed the highest yield of 1,2-epoxycyclohexane (**1b**): 88% yield, 97% selectivity to **1b**, and $\geq 99\%$ efficiency of H_2O_2 utilization (Table 1, entry 1). In this case, the turnover frequency (TOF) was as high as 210 h^{-1} .^{24–26} Epoxidation at ambient temperature also proceeded efficiently and gave **1b** in 84% yield (Table 1, entry 2). Oxidation did not proceed in the absence of the catalyst (Table 1, entry 3). The catalyst precursors of H_2WO_4 , H_2SeO_4 , and a mixture of H_2WO_4 and H_2SeO_4 were almost inactive for epoxidation (Table 1, entries 4–6). Selenium oxide, which has been applied to various oxidations with H_2O_2 , also showed low catalytic activity and selectivity to **1b** under the present conditions (Table 1, entry 7).²⁷ The reaction rate of **I** was 20 times larger than that of the simple dinuclear peroxotungstate $(\text{TBA})_2[\{\text{WO}(\text{O}_2)_2\}_2(\mu\text{-O})]$ (**W**₂), suggesting that the dimeric peroxotungstate unit is strongly activated by connection with the SeO_4^{2-} ligand (Table 1, entry 8). Epoxidation was carried out in the presence of various peroxotungstates with assembling ligands, $(\text{THA})_3[\text{XO}_4\{\text{WO}(\text{O}_2)_2\}_4]$ ($\text{THA} = [(n\text{-C}_6\text{H}_{13})_4\text{N}]^+$) [**AsW**₄, X = As; **PW**₄, X = P], $(\text{TBA})_2[\text{HXO}_4\{\text{WO}(\text{O}_2)_2\}_2]$ [**AsW**₂, X = As; **PW**₂, X = P], $(\text{TBA})_2[\text{SO}_4\{\text{WO}(\text{O}_2)_2\}_2]$ (**SW**₂), and $(\text{TBA})_2[\text{Ph}_2\text{SiO}_2\{\text{WO}(\text{O}_2)_2\}_2]$ (**SiW**₂). The reactivities were strongly dependent on the kinds of heteroatoms and the number of

(24) (a) Bruijninx, P. C. A.; Buurmans, I. L. C.; Gosiewska, S.; Moelands, M. A. H.; Lutz, M.; Spek, A. L.; Koten, G.; Gebbink, R. J. M. *K. Chem.—Eur. J.* **2008**, *14*, 1228. (b) Koo, D. H.; Kim, M.; Chang, S. *Org. Lett.* **2005**, *7*, 5015. (c) van Vliet, M. C. A.; Arends, I. W. C. E.; Sheldon, R. A. *Chem. Commun.* **1999**, 263. (d) Srinivas, K. A.; Kumar, A.; Chauhan, S. M. S. *Chem. Commun.* **2002**, 2456. (e) Rudolph, J.; Reddy, K. L.; Chiang, J. P.; Sharpless, K. B. *J. Am. Chem. Soc.* **1997**, *119*, 6189.

(25) (a) Berardi, S.; Bonchio, M.; Carraro, M.; Conte, V.; Sartorel, A.; Scorrano, G. *J. Org. Chem.* **2007**, *72*, 8954. (b) Nam, W.; Oh, S.-Y.; Sun, Y. J.; Kim, J.; Kim, W.-K.; Woo, S. K.; Shin, W. *J. Org. Chem.* **2003**, *68*, 7903. (c) Maiti, S. K.; Malik, K. M. A.; Gupta, S.; Chakraborty, S.; Ganguli, A. K.; Mukherjee, A. K.; Bhattacharyya, R. *Inorg. Chem.* **2006**, *45*, 9843. (d) Rowland, J. M.; Olmstead, M.; Mascharak, P. K. *Inorg. Chem.* **2001**, *40*, 2810. (e) van Vliet, M. C. A.; Arends, I. W. C. E.; Sheldon, R. A. *Chem. Commun.* **1999**, 821. (f) Srinivas, K. A.; Kumar, A.; Chauhan, S. M. S. *Chem. Commun.* **2002**, 2456. (g) Brinksma, J.; Hage, R.; Kerschner, J.; Feringa, B. L. *Chem. Commun.* **2000**, 537.

(26) The TOF was higher than those reported for the H_2O_2 -based catalytic systems for the epoxidation of cyclohexene (Table S2 in the Supporting Information).^{24,25} $[\text{Fe}^{\text{II}}(\text{PrLi})_2](\text{OTf})_2$ [PrLi = propyl 3,3-bis(1-methylimidazol-2-yl)-propionate, 4 h^{-1}],^{24a} $\text{WO}_3/\text{MCM-48}$ (2 h^{-1}),^{24b} $\text{Mn}(\text{TDCPP})\text{Cl}/\text{imidazole}$ [$\text{TDCPP} = 5,10,15,20\text{-tetrakis}(2',6'\text{-dichlorophenyl})\text{porphyrin}$, 78 h^{-1}],^{5a} $\alpha\alpha\beta\alpha\text{-(NaOH)}_2(\text{Fe}^{\text{III}}\text{OH}_2)(\text{P}_2\text{W}_{15}\text{O}_{56})_2^{14-}$ (2 h^{-1}),^{14g} $[(\text{MnOH})_2\text{Mn}_2\text{PW}_9\text{O}_{34}(\text{PW}_6\text{O}_{26})]^{17-}$ (8 h^{-1}),^{14c} perfluoroheptadecan-9-one (48 h^{-1}),^{24c} Ta-SBA-15 (41 h^{-1}),^{24d} and $\text{CH}_3\text{ReO}_3/\text{pyridine}$ (32 h^{-1}).^{24e} While the TOFs of $[\gamma\text{-SiW}_{10}\text{O}_{36}(\text{PhPO})_2]^{4-}$ (1200 h^{-1}),^{25a} $\text{Fe}(\text{tpfpp})\text{Cl}$ ($\text{tpfpp} = \text{meso-tetrakis(pentafluorophenyl)porphinate dianion}$, 2160 h^{-1}),^{25b} $[\text{MoO}(\text{O}_2)(\text{BOTH})_2]$ ($\text{BOTH} = N\text{-benzoylhydroxamic acid}$, 4550 h^{-1}),^{25c} $[\text{Fe}(\text{PaPy}_3)(\text{CH}_3\text{CN})](\text{ClO}_4)_2$ ($\text{PaPy}_3 = N,N\text{-bis}(2\text{-pyridylmethyl})\text{amine-}N\text{-ethyl-2-pyridine-2-carboxamide}$, 276 h^{-1}),^{25d} MTO (500 h^{-1}),^{25e} $[\text{Cl}_8\text{TPP-S}_4\text{Fe}^{\text{III}}]$ ($\text{Cl}_8\text{TPP-S}_4 = \text{tetrakis}(2',6'\text{-dichloro-3'-sulfonatophenyl})\text{porphyrinato}$, 420 h^{-1}),^{25f} and $\text{Mn}_2\text{O}(\text{OAc})_2(\text{TPTN})$ ($\text{TPTN} = N,N,N',N'\text{-tetrakis}(2\text{-pyridylmethyl})\text{propane-1,3-diamine}$, 217 h^{-1})^{25g} were higher than that of **I**, the use of excess additives and H_2O_2 , specific solvents and ligands, and microwave is required.

(27) Młochowski, J.; Brzłaszcz, M.; Giurg, M.; Palus, J. H.; Wójtowicz *Eur. J. Org. Chem.* **2003**, 4329.

(18) Vogel, A. I. *A Textbook of Quantitative Inorganic Analysis Including Elementary Instrumental Analysis*; Longman: New York, 1978.

(19) Murahashi, S.-I.; Mitsui, H.; Shiota, T.; Tsuda, T.; Watanabe, S. *J. Org. Chem.* **1990**, *55*, 1736.

(20) Paolucci, C.; Mazzini, C.; Fava, A. *J. Org. Chem.* **1995**, *60*, 169.

(21) Becke, A. D. *J. Chem. Phys.* **1993**, *98*, 1372.

(22) Hay, P. J.; Wadt, W. R. *J. Chem. Phys.* **1985**, *82*, 270.

(23) Frisch, M. J. et al. *Gaussian 03*, revision D.02; Gaussian, Inc.: Wallingford, CT, 2004.

Table 1. Effect of Catalysts and Solvents on the Epoxidation of Cyclohexene (**1a**) with 30% Aqueous H₂O₂^a

entry	catalyst	solvent	yield (%)	selectivity (%)				H ₂ O ₂ efficiency (%)
				1b	1c	1d	1e	
1	I	acetonitrile	88	97	<1	<1	3	>99
2 ^b	I	acetonitrile	90	93	<1	1	6	99
3	without	acetonitrile	<1					
4 ^c	H ₂ WO ₄	acetonitrile	8	99	<1	<1	<1	75
5 ^d	H ₂ SeO ₄	acetonitrile	<1	<1	<1	<1	99	>99
6 ^{c,d}	H ₂ SeO ₄ + H ₂ WO ₄	acetonitrile	<1	<1	<1	<1	99	16
7 ^e	SeO ₂	acetonitrile	5	82	17	<1	<1	99
8	W ₂	acetonitrile	11	99	<1	<1	<1	>99
9 ^f	I	acetonitrile	35	98	<1	<1	2	96
10 ^f	AsW ₄	acetonitrile	31	99	<1	<1	<1	99
11 ^f	SW ₂	acetonitrile	18	99	<1	<1	<1	92
12 ^f	PW ₄	acetonitrile	10	99	<1	<1	<1	99
13 ^f	AsW ₂	acetonitrile	4	99	<1	<1	<1	>99
14 ^f	PW ₂	acetonitrile	2	99	<1	<1	<1	>99
15 ^f	SiW ₂	acetonitrile	1	99	<1	<1	<1	>99
16	(TBA) ₄ [γ-SiW ₁₀ O ₃₄ (H ₂ O) ₂]	acetonitrile	60	99	<1	<1	1	90
17 ^g	(TBA) ₄ [γ-H ₂ SiV ₂ W ₁₀ O ₄₀]	acetonitrile	16	89	4	3	4	28
18	I	1,2-dichloroethane	64	83	<1	<1	17	81
19	I	<i>n</i> -butyronitrile	62	78	<1	<1	22	76
20	I	chloroform	52	93	<1	<1	7	90
21	I	dichloromethane	36	77	<1	<1	23	82
22	I	ethyl acetate	33	75	<1	<1	25	80
23	I	dimethoxyethane	19	94	<1	<1	6	96
24	I	dimethylformamide	1	99	<1	<1	<1	21
25	I	toluene	1	99	<1	<1	<1	>99

^a Reaction conditions: catalyst (**W**: 2 mol % with respect to H₂O₂), **1a** (5 mmol), 30% aqueous H₂O₂ (1 mmol), solvent (6 mL), 323 K, 40 min. Yield (%) = products (mol)/H₂O₂ used (mol) × 100. ^b 305 K, 120 min. ^c H₂WO₄ (1 mol % with respect to H₂O₂). ^d H₂SeO₄ (1 mol % with respect to H₂O₂). ^e SeO₂ (1 mol % with respect to H₂O₂). ^f 10 min. ^g Acetonitrile/*tert*-butyl alcohol (3 mL/3 mL).

W atoms, respectively. The yields of **1b** decreased in the order of **I** (35%) > **AsW**₄ (31%) > **SW**₂ (18%) > **PW**₄ (10%) > **AsW**₂ (4%) > **PW**₂ (2%) > **SiW**₂ (1%) (Table 1, entries 9–15). Such a reactivity order was also observed for stoichiometric epoxidation with the peroxotungstates. Therefore, the nature of the heteroatoms in the peroxotungstates is crucial in controlling the Lewis acidity of the peroxotungstates, which significantly affects their electrophilic oxygen-transfer reactivity.^{15,28,29} The yields and efficiencies of H₂O₂ utilization of divacant polyoxotungstate (TBA)₄[γ-SiW₁₀O₃₄(H₂O)₂]^{13a} and divanadium-substituted polyoxotungstate (TBA)₄[γ-H₂SiV₂W₁₀O₄₀]^{3b} were lower than those of **I** under the present conditions (Table 1, entries 16 and 17). Epoxidation of **1a** with H₂O₂ catalyzed by **I** was carried out in various solvents. Among the solvents tested,

acetonitrile was the most effective (Table 1, entries 1 and 18–25). No formation of acetamide was observed, showing that epoxidation does not proceed via a peroxy-carboximide intermediate generated by the reaction of acetonitrile with H₂O₂.³⁰ Biphasic 1,2-dichloroethane, chloroform, dichloromethane, and ethyl acetate systems and a homogeneous *n*-butyronitrile system showed moderate activities, while the selectivity to **1b** and efficiency of H₂O₂ utilization were lower than those of the acetonitrile system (Table 1, entries 1 and 18–22). Toluene, in which **I** was not soluble, and *N,N*-dimethylformamide were poor solvents (Table 1, entries 24 and 25).

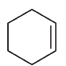
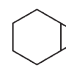
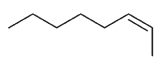
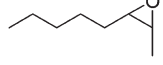

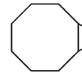
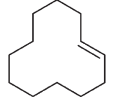
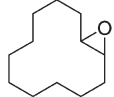


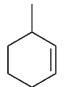
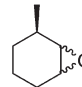
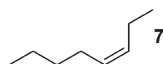
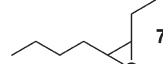
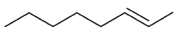
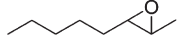
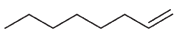
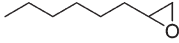
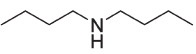
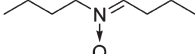
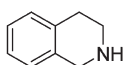
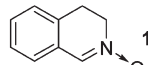
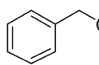
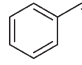
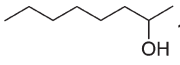
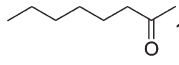
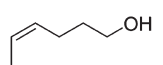
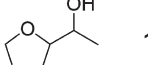
Table 2 shows the results of oxidation of various kinds of organic substrates with 30% aqueous H₂O₂ catalyzed by **I**. Epoxidation proceeded selectively to form the corresponding epoxides without the significant formation of allylic oxidation products and the hydrolysis, cleavage, and rearrangement of epoxides. Cyclic and internal olefins **1a–8a** were oxidized to the corresponding epoxides **1b–8b** in 87–99% yield with 96–99% selectivity and 91–99% efficiency of H₂O₂ utilization (Table 2, entries 1, 2, 4, 8, and 10–13). For epoxidation of *cis*- and *trans*-octenes **2a**, **7a**, and **8a**, the configuration around the C=C moiety was retained in the corresponding epoxides (Table 2, entries 2, 3, 12, and 13). The *trans/cis* ratio (64:36) for the **I**-catalyzed epoxidation of **6a** was similar

(28) For catalytic epoxidation by d⁰ transition-metal catalysts, the oxidation states of the metal centers are not changed during catalysis. The metal centers function as Lewis acids by withdrawing electrons from the O–O bond and thus increasing the electrophilic character of the coordinated peroxide. Active catalysts are the metal centers with strong Lewis acidity.^{29a–c} The p*K*_a values of the ligands can be recognized as an index of the Lewis acidity of transition-metal complexes.^{29d} The activity (yield) order of the dinuclear peroxotungstates with XO₄^{3–} ligands (X = Se, S, P, As, and Si) was the same as that of the p*K*_a values of H₃XO₄, suggesting that the Lewis acidity of W atoms has an important role for epoxidation.

(29) (a) Thiel, W. R.; Eppinger, J. *Chem.—Eur. J.* **1997**, *3*, 696. (b) Arends, I. W. C. E.; Sheldon, R. A. *Top. Catal.* **2002**, *19*, 133. (c) Oyama, S. T. In *Mechanisms in Homogeneous and Heterogeneous Epoxidation Catalysis*; Oyama, S. T., Ed.; Elsevier: Amsterdam, The Netherlands, 2008; pp 1–99. (d) Nabavizadeh, S. M.; Rashidi, M. *J. Am. Chem. Soc.* **2006**, *128*, 351.

(30) Payne, G. B.; Deming, P. H.; Williams, P. J. *Org. Chem.* **1961**, *26*, 651.

Table 2. Oxidation of Various Substrates with 30% Aqueous H₂O₂ Catalyzed by **I**^a

entry	substrate	time (min)	product	yield (%)
1	 1a	70	 1b	88 (210)
2 3 ^{b,c}	 2a	50 900	 2b	97 (166) 79 (31)
4 5 ^b 6 ^d 7 ^{d,e}	 3a	30 320 100 100	 3b	>99 (237) 94 (27) 99 96
8 ^f 9 ^{b,c}	 4a	50 380	 4b	99 70 (17)
10	 5a	80	 5b	99
11	 6a	50	 6b	87 (135) <i>trans/cis</i> = 64/36
12	 7a	50	 7b	99 (160)
13	 8a	300	 8b	92 (31)
14 ^g	 9a	200	 9b	73
15 ^h	 10a	140	 10b	85 (240)
16 ^h	 11a	120	 11b	91 (270)
17	 12a	1600	 12b	46 (11)
18	 13a	4000	 13b	52 (5)
19 ⁱ	 14a	1500	 14b	91

^a Reaction conditions: **I** (1 mol % with respect to H₂O₂), substrate (5 mmol), 30% aqueous H₂O₂ (1 mmol), acetonitrile (6 mL), 323 K. Yields were determined by GC and ¹H NMR. Yield (%) = product (mol)/H₂O₂ used (mol) × 100. The values in parentheses were TOF (h⁻¹). The TOF values were determined from the reaction profiles at low conversion (≤10%) of H₂O₂. ^b Substrate (1 mmol). ^c 313 K. ^d 298 K. ^e Recovered **I** (1 mol % with respect to H₂O₂; see the Supporting Information). ^f CH₃CN (9 mL). ^g **I** (5 mol % with respect to H₂O₂). ^h Substrate (1 mmol), 30% aqueous H₂O₂ (2 mmol), 305 K. ⁱ Substrate (1 mmol), 305 K.

to those for **W**₂ and **PW**₄ (Table 2, entry 11).^{13c} High yields and selectivities to the corresponding epoxides were also observed for epoxidation of **2a**, **3a**, and **4a** even with 1 equiv of H₂O₂ (**I**:substrate:H₂O₂ = 1:100:100; Table 2, entries 3, 5, and 9). Epoxidation proceeded at ambient temperature (Table 2, entry 6). Nonactivated terminal olefin **9a** was converted to **9b** in 73% yield (Table 2, entry 14). Secondary amines such as dibutylamine (**10a**) and tetrahydroisoquinoline (**11a**) were oxidized to the corresponding nitrones in good yield by using stoichiometric amounts of H₂O₂ with respect to the substrates (Table 2, entries 15 and 16). The present system showed moderate activity for oxidation of alcohols **12a** and **13a** (Table 2, entries 17

and 18), and the selectivities to the corresponding aldehyde and ketone were ≥95%. Oxidation of bis(homoallylic alcohol) **14a** gave the tetrahydrofuran derivative in 91% yield, while homoallylic and allylic alcohols were epoxidized selectively in the present system (Table 2, entry 19). This is probably due to rearrangement of the epoxide intermediate into the tetrahydrofuran derivative. Such an isomerization was also observed in the *m*-chloroperbenzoic acid, methyltrioxorhenium/H₂O₂, and titanosilicate/H₂O₂ systems.³¹

(31) Hartung, J.; Greb, M. *J. Organomet. Chem.* **2002**, 661, 67.

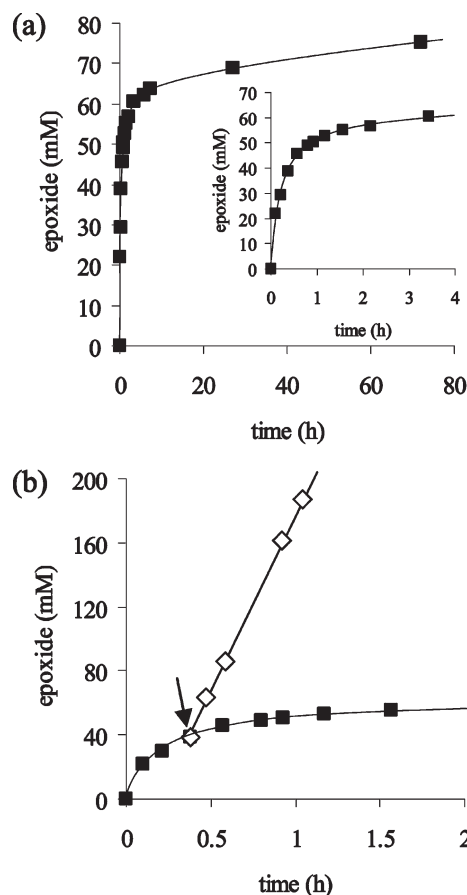


Figure 2. Reaction profiles for stoichiometric epoxidation of **3a** with **I**. (a) Reaction conditions: **I** (38 mM), **3a** (380 mM), CH₃CN (2.5 mL), 273 K. (b) After 20 min (i.e., 1 equiv of **3b** with respect to **I** was formed), 30% aqueous H₂O₂ (380 mM) was added, as indicated by an arrow.

Reaction Mechanism. The stability of **I** during catalytic epoxidation was investigated. The ⁷⁷Se NMR spectra of **I** both during and after the epoxidation of **3a** showed a signal at 1046 ppm, which was observed for the as-synthesized **I** (Figure S7 in the Supporting Information). In addition, **I** could easily be recovered in 98% yield by the addition of an excess amount of diethyl ether (precipitation method) to the reaction solution. The recovered **I** could be reused without loss of its catalytic activity and selectivity (Table 2, entries 6 and 7). These facts show that **I** is stable under the reaction conditions.

Stoichiometric epoxidation of **3a** (1 mmol) with **I** (100 μmol) at 273 K produced 198 ± 4 μmol of **3b** (Figure 2a), suggesting that **I** has 2 equiv of active oxygen for epoxidation. Such a stoichiometry is also observed for stoichiometric epoxidation of (*R*)-(+)-limonene with the di- and tetranuclear peroxotungstates with XO₄ⁿ⁻ ligands (X = S^{VI}, As^V, P^V, etc.).^{12h} After 1 equiv of **3b** with respect to **I** was formed, several ⁷⁷Se NMR signals at 1071, 1053, 1046, and 1019 ppm with an intensity ratio of 2:5:2:1 were observed, respectively (Figure 3b). Upon the addition of H₂O₂ (10 equiv with respect to **I**), these signals at 1071, 1053, and 1019 ppm almost disappeared and a signal at 1046 ppm assignable to **I** appeared again (Figure 3c). In this case, catalytic epoxidation of **3a** proceeded at almost the same rate (3.67 ± 0.20 mM min⁻¹) as that (3.72 ± 0.10 mM min⁻¹) under the stoichiometric conditions (Figure 2b). Several subsequent peroxo species such

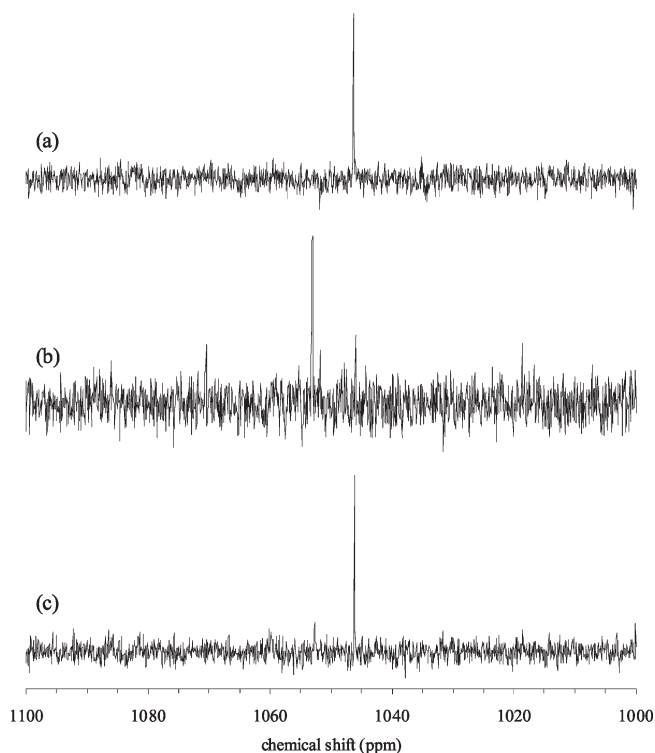


Figure 3. ⁷⁷Se NMR spectra of (a) **I**, (b) **I** after 1 equiv of **3b** with respect to **I** was formed, and (c) sample b with the addition of 30% H₂O₂ (380 mM). Reaction conditions: **I** (38 mM), **3a** (380 mM), CD₃CN (2.5 mL), 273 K.

as phosphorus-containing di-, tri-, and tetranuclear peroxotungstates, [PW_xO_y]^{z-} (x = 2–4), are also observed for stoichiometric epoxidation of **9a** with PW₄, and PW₄ is regenerated by reaction of the subsequent peroxo species with excess amounts of H₂O₂.^{12d} The signals at 1071, 1053, and 1019 ppm are probably assignable to subsequent peroxo species (**II**) such as [SeW_mO_n]^{o-} (m = 1 and 2) formed by the reaction of **I** with an olefin. Compound **I** is regenerated by the reaction of **II** with H₂O₂, and epoxidation proceeds catalytically.³² The ratio of the reaction rate of **II** to that of **I** was estimated to be 0.07 ± 0.01 from the reaction profile (Figure 2a). As was previously mentioned, **I** was the dominant species under steady-state turnover conditions (Figure S7 in the Supporting Information). The kinetics for epoxidation of **3a** with H₂O₂ catalyzed by **I** were investigated. The first-order dependence of the reaction rates on the concentrations of **I** (0.29–2.29 mM) and **3a** (0.07–0.86 M) and the zero-order dependence of the reaction rate on the concentration of H₂O₂ (0.04–0.36 M) were observed (Figures 4a–c and S8 in the Supporting Information). The reaction rate for epoxidation of *cis*-2-hexene at 313 K with 30% H₂O₂ under the conditions in Table 2 was 0.46 (0.04 mM min⁻¹) and almost the same as that (0.43 ± 0.02 mM min⁻¹) with 96% H₂O₂, suggesting that the reaction rates are not dependent on the concentration of water. All of these results suggest that **I** is the active species for

(32) After 2 equiv of **3b** with respect to **I** was formed, 10 equiv of H₂O₂ with respect to **I** was added to the reaction solution. The catalytic epoxidation rate (0.18 ± 0.01 mM min⁻¹) was much smaller than that (3.72 ± 0.10 mM min⁻¹) under the stoichiometric conditions, and a ⁷⁷Se NMR signal at 1046 ppm was not observed. All of these kinetic and NMR results suggest that epoxidation with **II** leads to irreversible catalyst inactivation.

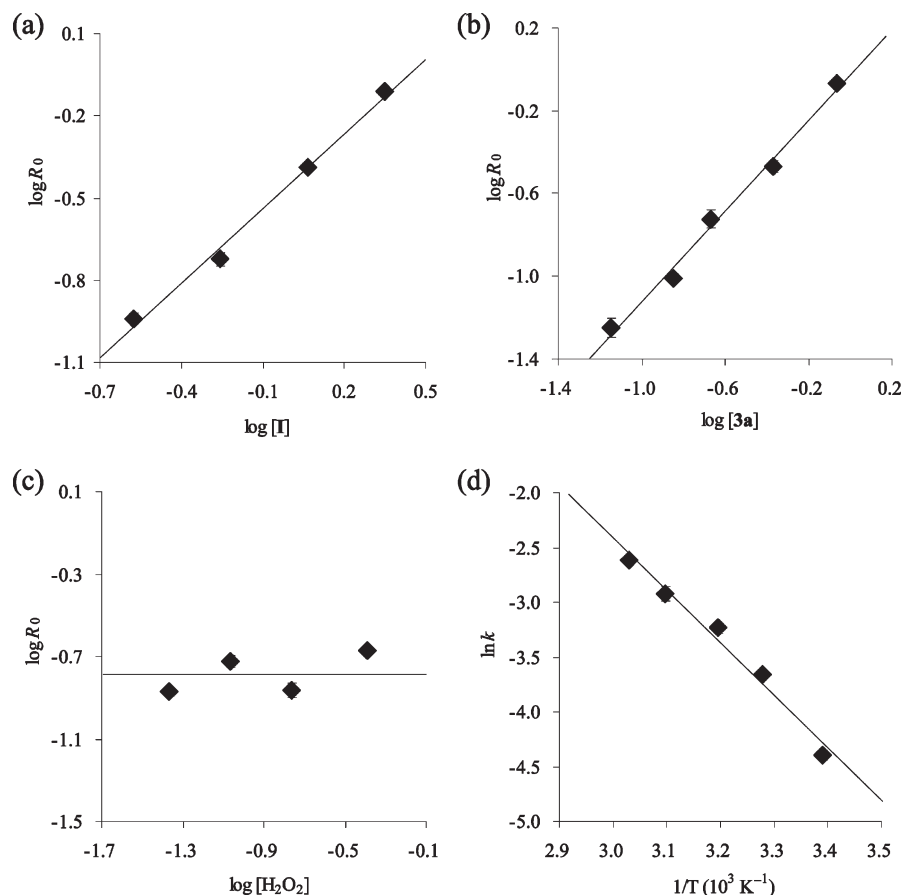
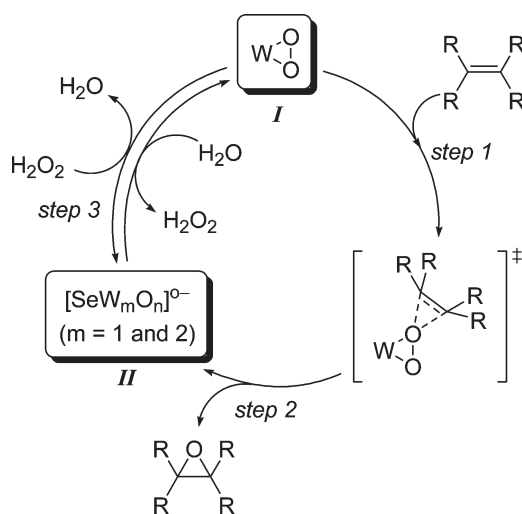


Figure 4. Dependence of the reaction rates on the concentrations of (a) **I**, (b) **3a**, and (c) H_2O_2 and (d) Arrhenius plots for epoxidation of **1a** with H_2O_2 catalyzed by **I**. Reaction conditions for part a: **I** (0.29–2.29 mM), **3a** (0.21 M), H_2O_2 (0.09 M), H_2O (0.38 M), acetonitrile (7 mL), 305 K. Slope = 0.91 ($R^2 = 0.99$). Reaction conditions for part b: **I** (0.57 mM), **3a** (0.07–0.86 M), H_2O_2 (0.09 M), H_2O (0.38 M), acetonitrile (7 mL), 305 K. Slope = 1.10 ($R^2 = 0.99$). Reaction conditions for part c: **I** (0.57 mM), **3a** (0.21 M), H_2O_2 (0.04–0.36 M), H_2O (0.38 M), acetonitrile (7 mL), 305 K. Reaction conditions for part d: **I** (0.57 mM), **3a** (0.21 M), H_2O_2 (0.09 M), H_2O (0.38 M), acetonitrile (7 mL), 295–330 K. Line fit: $\ln k = -4794/T + 11.96$ ($R^2 = 0.98$). R_0 values were determined from the reaction profiles at low conversions (< 10%) of both **3a** and H_2O_2 . Reaction profiles are shown in Figure S8 in the Supporting Information.

epoxidation and that the reaction of an olefin with **I** is the rate-determining step.

On the basis of these results, the present epoxidation of olefins possibly proceeds as follows (Scheme 1): First, the olefin directly attacks the peroxy oxygen groups to form the corresponding epoxide and subsequent peroxy species **II** (steps 1 and 2). Then, **I** is regenerated by the reaction of **II** with H_2O_2 (step 3). The dependence of the reaction rate on the reaction temperature (Arrhenius plots, 295–330 K) was investigated (Figure 4d). The good linearity of the Arrhenius plots was observed to afford the following activation parameters: $E_a = 39.8 \text{ kJ mol}^{-1}$, $\ln A = 12.0$, $\Delta H^\ddagger_{298 \text{ K}} = 37.4 \text{ kJ mol}^{-1}$, $\Delta S^\ddagger_{298 \text{ K}} = -153.6 \text{ J mol}^{-1} \text{ K}^{-1}$,

Scheme 1. Proposed Mechanism of the **I**-Catalyzed Epoxidation of Olefin with H_2O_2



(33) The kinetics for the epoxidation of **1a** with H_2O_2 catalyzed by **I** also showed the first-order dependence of the reaction rates on the concentrations of **I** (0.29–2.29 mM) and **1a** (0.07–0.86 M) and the zero-order dependence of the reaction rate on the concentration of H_2O_2 (0.04–0.36 M) (Figure S9a–c in the Supporting Information). In addition, the rate of the stoichiometric epoxidation of **1a** (160 mM) with **I** (8 mM) at 273 K was $0.31 \pm 0.02 \text{ mM min}^{-1}$ and agreed well with that ($0.32 \pm 0.01 \text{ mM min}^{-1}$) of the catalytic epoxidation of **1a** (160 mM) with H_2O_2 (160 mM) at 273 K by **I** (8 mM). The following activation parameters were afforded for the catalytic epoxidation of **1a** (Figure S9d in the Supporting Information): $E_a = 40.2 \text{ kJ mol}^{-1}$, $\ln A = 12.1$, $\Delta H^\ddagger_{298 \text{ K}} = 37.7 \text{ kJ mol}^{-1}$, $\Delta S^\ddagger_{298 \text{ K}} = -152.8 \text{ J mol}^{-1} \text{ K}^{-1}$, and $\Delta G^\ddagger_{298 \text{ K}} = 83.2 \text{ kJ mol}^{-1}$. The kinetics and activation parameters with **1a** were almost the same as those with **3a**, suggesting that the mechanism of epoxidation of **1a** is the same as that of **3a**.

and $\Delta G^\ddagger_{298 \text{ K}} = 83.1 \text{ kJ mol}^{-1}$.³³ The present activation energy is lower than those reported for tungsten-catalyzed epoxidation (e.g., 86.4 kJ mol^{-1} for Na_2WO_4 , 54.2 kJ mol^{-1} for PW_4 , and 55.9 – 68.2 kJ mol^{-1} for $\text{K}_2[\{\text{WO}(\text{O}_2)_2(\text{H}_2\text{O})\}_2(\mu\text{-O})] \cdot 2\text{H}_2\text{O}$), indicating the high reactivity of **I**

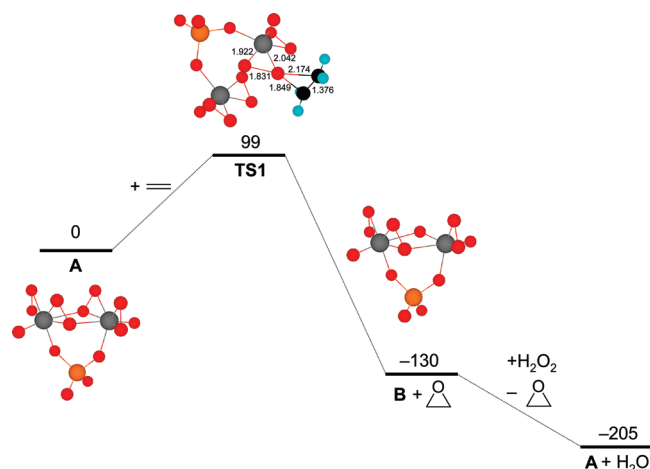


Figure 5. Calculated energy diagram of the epoxidation of ethylene to ethylene oxide by **I** in the gas phase (energies and lengths are in kJ mol^{-1} and Å, respectively). Orange, gray, red, black, and light-blue balls represent Se, W, O, C, and H atoms, respectively.

for epoxidation.^{12f,34} The negative value of the activation entropy $\Delta S^\ddagger_{298\text{ K}}$ suggests that a bimolecular transition state (electrophilic attack of a peroxo O atom at the C=C bond) is included in the rate-determining step.^{33,35}

In order to investigate the proposed reaction mechanism, the density functional theory calculations were carried out at the B3LYP/LanL2DZ+6-31+G(d,p) level. First, the reactivities of four kinds of peroxo O atoms (O1, O2, O3, and O4) in **I** for epoxidation were investigated. The transition-state structures and activation barriers for the epoxidation of ethylene with **I** were calculated on the assumption that the olefin double bond directly attacks the peroxo oxygen groups in a spiro fashion (i.e., the CCO plane is almost orthogonal to the WOO plane). The transition-state structures and the corresponding activation barriers are shown in Figure S6 in the Supporting Information.

(34) (a) Allan, G. G.; Neogi, A. N. *J. Catal.* **1976**, *16*, 197. (b) Jian, X.; Hay, A. S. *J. Polym. Sci., Part A: Polym. Chem.* **1991**, *29*, 547.

(35) Connors, K. A. *Chemical Kinetics, The Study of Reaction Rates in Solution*; VCH: New York, 1990.

The calculated activation barriers of an ethylene attack at O2 (**TS1**, 99 kJ mol^{-1}) was the lowest among those of ethylene attacks at O1 (**TS2**, 146 kJ mol^{-1}), O3 (**TS3**, 104 kJ mol^{-1}), and O4 (**TS4**, 106 kJ mol^{-1}), suggesting that an olefin attack at O2 would be the most favorable. The energies of the reaction steps were calculated according to Scheme 1, and the results are summarized in Figure 5. The formation of a subsequent peroxo species (**B**) and ethylene oxide by the reaction of ethylene with the selenium-containing dinuclear peroxotungstate (**A**) was calculated to be exothermic by -130 kJ mol^{-1} . The activation energy for the oxygen-transfer reaction (**TS1**) was calculated to be 99 kJ mol^{-1} . The H_2O_2 molecule reacted with **B** to form **A** and water, establishing the catalytic cycle. This step was calculated to be exothermic by -75 kJ mol^{-1} . Computational studies support that the oxygen-transfer step is the rate-determining step.

Conclusion

The dinuclear peroxotungstate with the SeO_4^{2-} ligand, **I**, was synthesized and characterized. Compound **I** showed high catalytic activity for the selective oxidation of various kinds of organic substances such as olefins, alcohols, and amines with H_2O_2 as the sole oxidant. On the basis of the kinetic, mechanistic, and spectroscopic investigation, it was found that **I** is the active species in the present epoxidation and that oxygen transfer from **I** to the C=C double bond is the rate-determining step.

Acknowledgment. This work was supported by the CREST program of JST, the Global COE Program (Chemistry Innovation through Cooperation of Science and Engineering), the Development in a New Interdisciplinary Field Based on Nanotechnology and Materials Science Programs, and a Grant-in-Aid for Scientific Research from the Ministry of Education, Culture, Science, Sports, and Technology of Japan.

Supporting Information Available: Experimental details, Tables S1 and S2, and Figures S1–S10. This material is available free of charge via the Internet at <http://pubs.acs.org>.